Inorg. Chem. **2007**, *46*, 5642–5650

Electronic Structure of Neutral and Monoanionic Tris(benzene-1,2-dithiolato)metal Complexes of Molybdenum and Tungsten

Ruta R. Kapre,[†] Eberhard Bothe,[†] Thomas Weyhermüller,[†] Serena DeBeer George,[‡] and Karl Wieghardt*,[†]

Max-Planck-Institut für Bioanorganische Chemie, Stiftstrasse 34-36, D-45470 Mülheim an der Ruhr, Germany, and Stanford Synchroton Radiation Laboratory, SLAC, Stanford University, Stanford, California 94309

Received March 30, 2007

The reaction of 3 equiv of the ligand 2-mercapto-3,5-di-*tert*-butylaniline, $H_2[L_{N,S}]$, or 3,5-di-*tert*-butyl-1,2-benzenedithiol, $H_2[L_{S,S}]$, with 1 equiv of $[MoO_2(acac)_2]$ or WCl_6 (acac = acetonylacetate(1-)) in methanol or CCl_4 afforded the diamagnetic neutral complexes $[Mo^V(L_{N,S})_2(L^{\bullet}_{N,S})]^0$ (**1**), $[Mo^V(L_{S,S})_2(L^{\bullet}_{S,S})]$ (**2**), and $[W^V(L_{S,S})_2(L^{\bullet}_{S,S})]$ (**3**), where $(L^{\bullet}_{N,S})^-$ and $(L^{\bullet}_{S,S})^-$ represent monoanionic π-radical ligands ($S_{rad} = {}^1/_2$), which are the one-electron oxidized forms of the corresponding closed-shell dianions $(L_{N,S})^{2-}$ and $(L_{S,S})^{2-}$. Complexes **1**–**3** are trigonal-prismatic members of the electron-transfer series $[ML_3]^z$ ($z = 0, 1-, 2-$). Reaction of **2** and **3** with $[N(n\text{-}Bu)_4](SH)$ in CH_2Cl_2 under anaerobic conditions afforded paramagnetic crystalline $[N(n\text{-}Bu)_4][Mo^V(L_{S,S})_3]$ (**4**) and $[N(n\text{-}Bu)_4][W^V(L_{S,S})_3]$ (**5**). Complexes **1**–**5** have been characterized by X-ray crystallography. S K-edge X-ray absorption and infrared spectroscopy prove that a π-radical ligand $(L^{\bullet}_{S,S})^-$ is present in neutral **2** and **3,** whereas the monoanions $[M^V(L_{S,S})_3]^-$ contain only closed-shell dianionic ligands. These neutral species have previously been incorrectly described as $[M^{VI}(L)_3]^0$ complexes with a Mo^{VI} or W^{VI} (d^0) central metal ion; they are, in fact M^V (d^1) (M = Mo, W) species: $[Mo^V(L_{S,S})_2(L^{\bullet}_{S,S})]$ and $[W^V(L_{S,S})_2(L^{\bullet}_{S,S})]$ with a diamagnetic ground state $S_t = 0$, which is generated by intramolecular, antiferromagnetic coupling between the M^V (d^1) central ion ($S_M = {}^1/_2$) and a ligand π radical $(L^{\bullet}_{S,S})^-$ ($S_{rad} = {}^1/_2$).

Introduction

Since their original discovery in 1965,[1] it is well-established that tris(benzene-1,2-dithiolato)metal complexes of molybdenum and tungsten form an electron-transfer series where the neutral, monoanionic, and dianionic species $[M(bdt)_3]^z$ ($z = 0, 1-, 2-$) have been isolated and structurally characterized.[1−6] We will show here that the monocation $[M(bdt)_3]^+$ ($z = 1+$) may also be accessible, at least electrochemically.

From 1965 until today, the electronic structures of these members of the series have been discussed by nearly all authors in the following fashion: (1) The trigonal-prismatic, diamagnetic neutral complexes, $[M(bdt)_3]$, are considered to contain a Mo(VI) or W(VI) ion with a d^0 electron configuration and three closed-shell dianionic dithiolato(2-) ligands; (2) correspondingly, the one-electron reduced forms, namely, the paramagnetic monoanions $[M^V(bdt)_3]^-$, are considered to contain a Mo(V) (or W(V)) ion with a d^1 electron configuration ($S = {}^1/_2$); and finally (3), the dianions $[M^{IV}(bdt)_3]^{2-}$ contain a Mo(IV) or W(IV) central ion with a d^2 electron configuration ($S = 1$). Thus, the redox series has been

* To whom correspondence should be addressed. E-mail: wieghardt@mpi-muelheim.mpg.de.
[†] Max-Planck-Institut für Bioanorganische Chemie.
[‡] Stanford Synchroton Radiation Laboratory.

(1) (a) Smith, A. E.; Schrauzer, G. N.; Mayweg, V. P.; Heinrich, W. *J. Am. Chem. Soc.* **1965**, *87*, 5798. (b) Stiefel, E. I.; Eisenberg, R.; Rosenberg, R. C.; Gray, H. B. *J. Am. Chem. Soc.* **1966**, *88*, 2956.
(2) (a) $[Mo(bdt)_3]$: Cowie, M.; Bennett, M. J. *Inorg. Chem.* **1976**, *15*, 1584. (b) $[W(bdt)_3]$: Huynh, H. V.; Lügger, T.; Hahn, F. E. *Eur. J. Inorg. Chem.* **2002**, 3007.
(3) $[Mo(bdt)_3]^-$: (a) Cervilla, A.; Llopis, E.; Marco, D.; Perez, F. *Inorg. Chem.* **2001**, *40*, 6525. (b) Schulze-Isfort, C.; Pape, T.; Hahn, F. E. *Eur. J. Inorg. Chem.* **2005**, 2607. (c) Sellmann, D.; Zapf, L. *Z. Naturforsch., B: Chem. Sci.* **1985**, *40b*, 380.
(4) $[W(bdt)_3]^-$: (a) Borrow, T. E.; Morris, R. H.; Hills, A.; Hughes, D. L.; Richards, R. L. *Acta Crystallogr. Sect. C* **1993**, *49*, 1591. (b) Knoch, F.; Sellmann, D.; Kern, W. *Z. Kristallogr.* **1992**, *202*, 326.
(5) (a) $[Mo(bdt)_3]^{2-}$: ref 3b. (b) $[W(bdt)_3]^{2-}$: Lorber, C.; Donahue, J. P.; Goddard, C. A.; Nordlander, E.; Holm, R. H. *J. Am. Chem. Soc.* **1998**, *120*, 8102. (c) Knoch, F.; Sellmann, D.; Kern, W. *Z. Kristallogr.* **1993**, *205*, 300.
(6) $[M(bdtCl_2)_3]^{1-/2-}$ (M = Mo, W): Sugimoto, H.; Furukawa, Y.; Tarumizu, M.; Miyake, H.; Tanaka, K.; Tsukube, H. *Eur. J. Inorg. Chem.* **2005**, 3088.

10.1021/ic700600r CCC: $37.00
Published on Web 06/14/2007

Scheme 1

Ligands

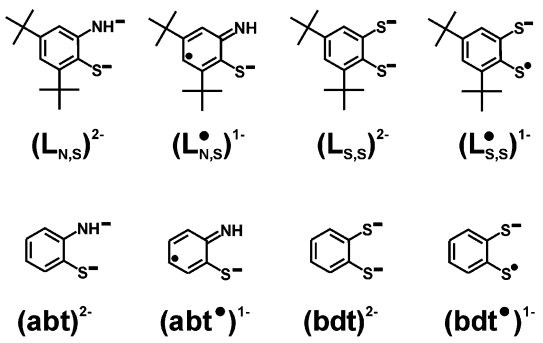

considered to involve metal-centered one-electron-transfer steps only as shown in eq 1.

$$[M(bdt)_3]^0 \underset{-e}{\overset{+e}{\rightleftarrows}} [M^{V}(bdt)_3]^- \underset{-e}{\overset{+e}{\rightleftarrows}} [M^{IV}(bdt)_3]^{2-} \qquad (M = Mo, W) \quad (1)$$

$E^1_{1/2}$ $E^2_{1/2}$

The geometry of the MS_6 polyhedron in these complexes has been discussed at various levels of sophistication to understand the trigonal-prismatic arrangement in neutral $[M(bdt)_3]^0$ (M = Mo, W) species. The monoanions display a more distorted geometry, which is intermediate between an octahedral and trigonal-prismatic geometry.

As Hahn et al. have recently shown, the dianion $[Mo^{IV}(bdt)_3]^{2-}$ possesses again a distorted trigonal-prismatic coordination geometry ($\theta = 24.8°$),[3b] whereas $[W^{IV}(bdt)_3]^{2-}$ is trigonal-prismatic ($\theta = 3.5°$).[5b]

These geometries have been interpreted controversially in either terms of electronic factors or packing forces in the solid state where the countercations are of importance.[3,6,7]

To elucidate the geometrical and electronic factors of this electron-transfer series, we have synthesized such tris(benzene-1,2-dithiolato)metal complexes of Mo and W using the sterically very bulky ligand 3,5-di-*tert*-butylbenzene-1,2-dithiol originally introduced by Sellmann et al.[8,9] as shown in Schemes 1 and 2. This choice should eliminate steric factors such as packing forces in the solid state.

For the first time, we show unequivocally by S K-edge X-ray absorption spectroscopy that the neutral complexes contain a Mo(V) ion, a ligand π-radical monoanion, and two closed-shell ligand dianions, $[M^{V}(L)_2(L^{\bullet})]^0$, whereas the paramagnetic monoanions $[M(L)_3]^-$ contain a central Mo(V) or W(V) ion (d^1) and three closed-shell, dianionic ligands.

Experimental Section

The ligands 2-mercapto-3,5-di-*tert*-butylaniline, $H_2[L_{N,S}]$, and 3,5-di-*tert*-butylbenzene-1,2-dithiol, $H_2[L_{S,S}]$ (Scheme 1), have been prepared as described in refs 8 and 9, respectively. The complex

Scheme 2

Complexes

$[Mo^{V}(L_{N,S})_2(L^{\bullet}_{N,S})]^0 \cdot (C_2H_5)O$	(S=0)	(1)
$[Mo^{V}(L_{S,S})_2(L^{\bullet}_{S,S})]^0$	(S=0)	(2)
$[W^{V}(L_{S,S})_2(L^{\bullet}_{S,S})]^0$	(S=0)	(3)
$[N(n\text{-}Bu)_4][Mo^{V}(L_{S,S})_3] \cdot CH_3CN$	(S=1/2)	(4)
$[N(n\text{-}Bu)_4][W^{V}(L_{S,S})_3] \cdot CH_3CN$	(S=1/2)	(5)

$[MoO_2(acac)_2]$ (acac$^-$ = acetonylacetonate(1-)) has been prepared according to ref 10.[10]

$[Mo^{V}(L_{N,S})_2(L^{\bullet}_{N,S})]\cdot(C_2H_5)_2O$ (1). To a solution of the ligand $H_2[L_{N,S}]$ (365 mg; 1.5 mmol) in methanol (15 mL) was added a solution of $[MoO_2(acac)_2]$ (164 mg; 0.5 mmol) in methanol (10 mL) at 20 °C. A color change to dark green was immediately observed. The solution was stirred for 1 h in the presence of air at 20 °C after which time a green precipitate of **1** was filtered off and recrystallized from a mixture of CH_2Cl_2/diethylether (1:1 vol). Yield: 320 mg (80%). Anal. Calcd for $C_{46}H_{73}N_3S_3OMo$: C, 62.9; H, 7.8; N, 5.2; Mo, 12.0. Found: C, 62.8; H, 7.9; N, 5.2; Mo, 12.1.

$[Mo^{V}(L_{S,S})_2(L^{\bullet}_{S,S})]$ (2). To a solution of the ligand $H_2[L_{S,S}]$ (127 mg; 0.5 mmol) in methanol (15 mL) was added a solution of $[MoO_2(acac)_2]$ (54 mg; 0.17 mmol) in methanol (10 mL). The color of the reaction mixture turned immediately to dark green. Within 1 h at 20 °C, a green precipitate had formed, which was filtered off and recrystallized from an CH_3CN/diethylether (1:1 vol) mixture. Yield: 112 mg (85%). Anal. Calcd for $C_{42}H_{60}S_6Mo$: C, 59.1; H, 7.1; S, 22.5; Mo, 11.24. Found: C, 58.9; H, 6.9; S, 22.3; Mo, 10.9.

$[W^{V}(L_{S,S})_2(L^{\bullet}_{S,S})]$ (3). To a solution of WCl_6 (56 mg; 0.13 mmol) in CCl_4 (20 mL) was added under anaerobic conditions a solution of the ligand $H_2[L_{S,S}]$ (100 mg; 0.39 mmol) in CCl_4 (10 mL) whereupon the color of the resulting solution changed to deep blue-green. After heating to reflux for 3 h under an Ar-blanketing atmosphere and cooling to 20 °C, the volume of the reaction mixture was reduced by one-half by evaporation. A blue-green powder formed, which was collected by filtration and recrystallized from an ethanol/diethylether (1:1 vol) mixture. Yield: 92 mg (70%). Anal. Calcd for $C_{42}H_{60}S_6W$: C, 53.6; H, 6.4; S, 10.4; W, 19.5. Found: C, 53.5; H, 6.5; S, 10.4; W, 19.7.

$[N(n\text{-}Bu)_4][Mo^{V}(L_{S,S})_3]\cdot CH_3CN$ (4·CH_3CN). To a solution of **2** (85 mg; 1.0 mmol) in CH_2Cl_2 (50 mL) was added $[N(n\text{-}Bu)_4]SH$ (28 mg; 1.0 mmol) under an Ar-blanketing atmosphere whereupon a color change from green to olive green was observed. The air-sensitive mixture was concentrated in vacuo by evaporation of the solvent, and the resulting solid was recrystallized from a mixture of CH_2Cl_2 and acetonitrile (1:1 vol). Yield: 94 mg (87%). Anal. Calcd for $C_{60}H_{99}N_2S_6Mo$: C, 59.1; H, 7.1; S, 22.5; Mo, 11.2. Found: C, 58.9; H, 6.9; S, 22.3; Mo, 10.9. μ_{eff} (30−300 K): 1.7 μ_B; $g_{||} = 2.0021$; $g_{\perp} = 2.0191$.

$[N(n\text{-}Bu)_4][W^{V}(L_{S,S})_3]\cdot CH_3CN$ (5·CH_3CN). This compound has been synthesized as described above for **4** by using **3** as the starting material. Yield: 102 mg (85%). Anal. Calcd for $C_{60}H_{99}N_2S_6W$: C, 58.85; H, 8.82; S, 15.7; W, 15.0. Found: C, 58.9; H, 8.2; S, 15.5; W, 15.3. μ_{eff} (20−300 K): 1.7 μ_B; $g_{||} = 1.9869$; $g_{\perp} = 2.00$.

X-ray Crystallographic Data Collection and Refinement of the Structures. A black single crystal of **1**·Et_2O and dark-brown-reddish crystals of **2**, **3**·0.5MeCN, **4**·MeCN, and **5**·0.2CH_2Cl_2 were

(7) Campbell, S.; Harris, S. *Inorg. Chem.* **1996**, *35*, 385.
(8) Sellmann, D.; Emig, S.; Heinemann, F. W.; Knoch, F. *Z. Naturforsch.* **1998**, *53b*, 1461.
(9) (a) Sellmann, D.; Freyberger, G.; Eberlein, R.; Böhlen, E.; Huttner, G.; Zsolnai, L. *J. Organomet. Chem.* **1987**, *323*, 21. (b) Sellmann, D.; Käppler, O. *Z. Naturforsch.* **1987**, *42b*, 1291.
(10) Kawamoto, T.; Kuma, H.; Kushi, Y. *Bull. Chem. Soc. Jpn.* **1997**, 1599.

Table 1. Crystallographic Data for **1**·Et_2O, **2**, **3**·0.5MeCN, **4**·MeCN, and **5**·0.2CH_2Cl_2

	1·Et_2O	**2**	**3**·0.5MeCN	**4**·MeCN	**5**·0.2CH_2Cl_2
formula	$C_{46}H_{73}MoN_3OS_3$	$C_{42}H_{60}MoS_6$	$C_{43}H_{61.5}N_{0.5}S_6W$	$C_{60}H_{99}MoN_2S_6$	$C_{58.2}H_{96.4}Cl_{0.4}NS_6W$
fw	876.19	853.20	961.64	1136.71	1199.49
space group	$P2_1/n$, No. 14	$P2_1/n$, No. 14	$P2_1/n$, No. 14	$P2_1/c$, No. 14	$P2_1/c$, No. 14
a, Å	13.8156(7)	13.3491(6)	10.7227(2)	14.5012(6)	14.5159(8)
b, Å	20.8414(9)	18.5592(8)	18.7101(4)	21.7374(9)	21.949(2)
c, Å	16.5381(8)	19.3158(8)	23.7213(8)	20.2212(9)	20.174(2)
β, deg	92.154(4)	99.663(5)	94.045(5)	90.563(5)	91.68(1)
V, Å	4758.6(4)	4717.6(4)	4747.2(2)	6373.8(5)	6424.9(9)
Z	4	4	4	4	4
T, K	100(2)	100(2)	100(2)	100(2)	100(2)
ρ calcd, g cm^{-3}	1.223	1.201	1.346	1.185	1.240
reflns collected/$2\Theta_{max}$	58033/52.00	111338/61.96	90719/52.70	83077/55.00	28186/45.00
unique reflns ($I > 2\sigma(I)$)	9327/7966	14979/11043	9679/9211	14617/11710	8319/6060
no. of params/restraints	529/21	489/31	516/3	627/1	617/13
λ, Å /μ(Kα), cm^{-1}	0.71073/4.42	0.71073/5.69	0.71073/27.25	0.71073/4.38	0.71073/20.24
R1[a]/GOF[b]	0.0546/1.155	0.0389/1.027	0.0340/1.133	0.0546/1.111	0.0510/1.089
wR2[c] ($I > 2\sigma(I)$)	0.1115	0.0756	0.0774	0.1004	0.0881
residual density, e·$Å^{-3}$	+0.95/−0.59	+0.77/−0.53	+1.67/−1.58	+0.81/−0.53	+0.83/−0.53

[a] Observation criterion: $I > 2\sigma(I)$. $R1 = \sum||F_o| - |F_c||/\sum|F_o|$. [b] $GOF = [\sum[w(F_o^2 - F_c^2)^2]/(n-p)]^{1/2}$. [c] $wR2 = [\sum[w(F_o^2 - F_c^2)^2]/\sum[w(F_o^2)^2]]^{1/2}$ where $w = 1/\sigma^2(F_o^2) + (aP)^2 + bP$, $P = (F_o^2 + 2F_c^2)/3$.

coated with perfluoropolyether, picked up with a glass fiber, and were immediately mounted in the nitrogen cold stream of the diffractometer to prevent loss of solvent. A Nonius Kappa-CCD diffractometer equipped with a Mo-target rotating-anode X-ray source and a graphite monochromator (Mo Kα, $\lambda = 0.71073$ Å) was used. Final cell constants were obtained from least-squares fits of all measured reflections. Crystal faces of all crystals, except those of **2**, were determined, and the Gaussian-type correction routine embedded in *XPREP*[11] was applied to correct the data sets for absorption. The structures were readily solved by direct and Patterson methods and subsequent difference Fourier techniques. The Siemens *SHELXTL*[11] software package was used for the solution and artwork of the structure, and *SHELXL97*[12] was used for the refinement. All non-hydrogen atoms were refined anisotropically. Hydrogen atoms were placed at calculated positions and refined as riding atoms with isotropic displacement parameters. Crystallographic data of the compounds are listed in Table 1.

Some disorder was observed in all five structures, and split-atom models were refined. Some residual electron density was found next to atoms in the first coordination spheres of **1**−**3**. Refinement of the split models revealed that the complexes coexist in the crystal in two different conformers, due to the bent binding mode of the three bidentate ligands giving the molecules a paddle-wheel character. The minor components were found to have contributions of about 5% for C_3 symmetric **1** and 11 and 13% for C_1 symmetric **2** and **3**, respectively. The acetronitrile solvent molecule in **3** is not fully occupied and disordered. Two split positions were refined with a ratio of 50:50 and a total occupation factor of 0.5. A solvent molecule of crystallization could not be localized in isostructural **2**. Compounds **4** and **5** are also isostructural, though **5** contains the remaining electron density of about 0.2CH_2Cl_2 and **4** crystallizes with a molecule of acetonitrile. The $[NBu_4]^+$ cations are disordered similarly in both cases, and a related split-atom model was used. All refinements of split positions were performed with applied restraints using the SADI and EADP instruction in *SADABS*.[13]

X-ray Absorption Spectroscopy. All data were measured at the Stanford Synchroton Radiation Laboratory under ring conditions of 3.0 GeV and 60−100 mA. S K-edge and Mo L-edge data were measured using the 54-pole wiggler beam line 6-2 in a high-magnetic field mode of 10 kG with a Ni-coated harmonic rejection mirror and a fully tuned Si(111) double-crystal monochromator. Details of the optimization of this setup for low-energy studies have been described previously. (Reference: Hedman, B.; Frank, P.; Gheller, S. F.; Roe, A. L.; Newton, W. E.; Hodgson, K. O. *J. Am. Chem. Soc.* **1988**, *110*, 3798.) Data were measured at room temperature by fluorescence using a Lytle detector. To check for reproducibility, 2−3 scans were measured for each sample. The S K− and Mo L-edge energies were calibrated using the S K-edge spectra of $Na_2S_2O_3$·$5H_2O$, run at intervals between sample scans. The maximum of the first pre-edge feature in the spectrum was fixed at 2472.02 eV. A step size of 0.08 eV was used over the edge region. Data were averaged, and a smooth background was removed from all spectra by fitting a polynomial to the pre-edge region and subtracting this polynomial from the entire spectrum. Normalization of the data was accomplished by fitting a flattened polynomial or straight line to the postedge region and normalizing the postedge to 1.0.

Physical Measurements. Electronic absorption spectra of the complexes and spectra from the spectroelectrochemical measurements were recorded on a HP 8452A diode array spectrophotometer (range of 200−1100 nm). Cyclic voltammograms (CVs) and coulometric electrochemical experiments were performed with an EG&G potentiostat/galvanostat. Solution infrared spectra of reduced species were measured by performing electrolysis (at −25 °C) in a electrochemical thin layer cell (OTTLE; $d = 0.18$ mm) equipped with a platinum-grid working electrode. The OTTLE was mounted in an FT infrared spectrophotometer (Perkin-Elmer, system 2000), thus allowing one to monitor the infrared spectral changes in situ during electrolysis.

Temperature-dependent (2−298 K) magnetization data were recorded with a SQUID magnetometer (MPMS Quantum Design) in an external magnetic field of 1 T. The experimental magnetic susceptibility data were corrected for underlying diamagnetism using tabulated Pascal's constants. X-band EPR spectra were recorded with a Bruker ESP 300 spectrometer.

Results and Discussion

1. Syntheses and Crystal Structures. From the reaction of 3 equiv of the ligand 2-mercapto-3,5-di-*tert*-butylaniline, $H_2(L_{N,S})$[8] and 1 equiv of $[MoO_2(acac)_2]$[10] in methanol in the presence of air, a dark-green microcrystalline precipitate of $[Mo(L_{N,S})_2(L^{\bullet}_{N,S})]$ (**1**) was obtained in good yield.

Complex **1** is diamagnetic; it possesses an $S = 0$ ground state. The molecular structure of the neutral complex in crystals of **1**·(diethylether) is shown in Figure 1. Table 2 summarizes selected bond distances and angles.

(11) *SHELXTL*, version 5; Siemens Analytical X-Ray Instruments, Inc.; Madison, Wisconsin, 1994.
(12) Sheldrick, G. M. *SHELXL97*; Universität Göttingen: Göttingen, Germany, 1997.
(13) *SADABS*, version 2004-1; Bruker-Nonius: Delft, The Netherlands.

Table 2. Selected Bond Distances (Å) and Angles (deg) in **1**·(diethylether)

Mo(1)−N(2)	2.026(3)	Mo(1)−N(22)	2.026(3)	Mo(1)−N(42)	2.024(3)
Mo(1)−S(1)	2.397(9)	Mo(1)−S(21)	2.385(9)	Mo(1)−S(41)	2.378(9)
S(1)−C(1)	1.741(3)	S(21)−C(21)	1.744(3)	S(41)−C(41)	1.737(3)
N(2)−C(2)	1.363(4)	N(22)−C(22)	1.370(4)	N(42)−C(42)	1.360(4)
C(1)−C(2)	1.421(4)	C(21)−C(22)	1.428(5)	C(41)−C(42)	1.427(5)
C(1)−C(6)	1.433(4)	C(21)−C(26)	1.435(4)	C(41)−C(46)	1.427(4)
C(2)−C(3)	1.416(4)	C(22)−C(23)	1.418(4)	C(42)−C(43)	1.410(5)
C(3)−C(4)	1.376(4)	C(23)−C(24)	1.367(5)	C(43)−C(44)	1.380(5)
C(4)−C(5)	1.422(4)	C(24)−C(25)	1.418(5)	C(44)−C(45)	1.415(5)
C(5)−C(6)	1.387(4)	C(25)−C(26)	1.380(5)	C(45)−C(46)	1.379(5)
N(42)−Mo(1)−S(41)	77.68(8)				
N(22)−Mo(1)−S(21)	73.99(8)				
N(2)−Mo(1)−S(1)	77.27(8)				
N(2)−Mo(1)−S(41)	132.93(8)				
N(22)−Mo(1)−S(41)	136.14(9)				
N(42)−Mo(1)−S(21)	134.36(9)				

Table 3. Twist Angles Θ (deg) for Complexes[a]

complex	Θ_1	Θ_2	Θ_3	Θ_{av}	ref
		neutral			
$[Mo(bdt)_3]$	0	0	0	0	2a
$[W(bdt)_3]$	0	0	0	0	2b
$[Mo(L_{S,S})_3]$	1.0	0.9	0.6	1.5	this work
$[W(L_{S,S})_3]$	0.5	2.4	0.1	1.0	this work
$[Mo(L_{N,S})_3]$	2.5	1.9	1.3	1.9	this work
		monoanion			
$[Mo(bdt)_3]^-$	35.6	34.4	30.4	33.5	3
$[W(bdt)_3]^-$	31.2	31.8	33.9	32.3	4
$[Mo(L_{S,S})_3]^-$	39.9	25.4	29.7	31.7	this work
$[W(L_{S,S})_3]^-$	37.9	26.3	30.3	31.5	this work
		dianion			
$[Mo(bdt)_3]^{2-}$	23.7	28.2	22.6	24.8	3b
$[W(bdt)_3]^{2-}$	3.5	1.8	0.4	1.9	5b

[a] Ideal trigonal-prismatic geometry $\Theta_{av} = 0°$, octahedral $\Theta_{av} = 60°$.

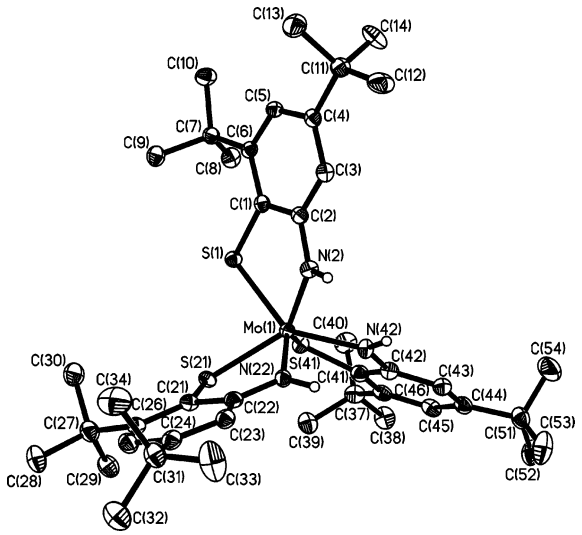

Figure 1. Structure of the neutral complex $[Mo(L_{N,S})_3]^0$ in crystals of **1**·(Et_2O). Small open circles represent hydrogen atoms of the NH groups. Thermal ellipsoids are drawn at the 50% level.

The neutral complex **1** consists of three bidentate, N,S-coordinated chelating ligands and a central molybdenum ion. The six donor atoms are bound in a nearly ideal trigonal-prismatic geometry. Two triangular faces can be defined, consisting of three sulfur atoms or of three nitrogen atoms, respectively. The three twist-angles, namely, N2−Mo−S1 at 2.6°, S21−Mo−N22 at 1.9°, and S41−Mo−N42 at 1.3°, are small and indicative of the nearly ideal trigonal-prismatic arrangement of the N_3S_3Mo polyhedron. This angle Θ is ideally 0° in a regular trigonal prism and 60° in a regular octahedron. Note that the descriptor Θ of the distortion in such tris-chelate complexes is a chelate projection (twist) angle. The projection along the C_3 axis normal to the mean planes defined by the above pair of triangular faces (N_3 and S_3) gives this angle Θ (Table 3). In $[Mo(abt)_3]$, the angle Θ is larger, at 12.4° on average.[14] The diethylether solvent molecule is hydrogen bonded to the neutral molecule **1** via an interaction N1−H1···O43 (N1···O43 = 3.019(4) Å).

The twist angle Θ of tris-chelate complexes is the chelate projection angle along the approximate C_3 axis normal to the two mean planes $\Theta_{av} = (\Theta_1 + \Theta_2 + \Theta_3)/3$ of two triangular faces defined by three sulfur atoms (one of each chelate).

It is now important to realize that the oxidation level of the ligand can vary from a closed-shell amidothiophenolate dianion, $(L_{N,S})^{2-}$, to a π-radical monoanion $(L^{\bullet}_{N,S})^{-}$.[15]

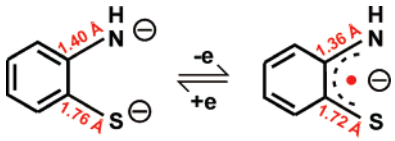

We have previously shown that the C−S and C−N bond distances are significantly different in both forms and, in addition, the aromatic phenyl ring in $(L_{N,S})^{2-}$ displays six nearly equidistant C−C bonds whereas the radical monoanion shows a quinoid-type distortion with two alternating short C−C bonds at ∼1.37 Å and four longer C−C bonds at ∼1.41 Å.[15]

The structure of **1** clearly shows that the presence of three amidothiophenolato(2-) ligands in **1** and $[Mo(abt)_3]$[14] can be ruled out since the observed C−S and C−N bonds are too short.

The shorter C−N and C−S bond lengths indicate the presence of at least one π radical. Thus, from the analysis of the structural data of **1** and $[Mo(abt)_3]$,[14] the following electronic structures may be viable: $[Mo^{V}(L_{N,S})_2(L^{\bullet}_{N,S})]^0$, $[Mo^{IV}(L_{N,S})(L^{\bullet}_{N,S})_2]^0$, or $[Mo^{III}(L^{\bullet}_{N,S})_3]^0$ and, similarly, $[Mo^{V}(abt)_2(abt^{\bullet})]$, $[Mo^{IV}(abt)(abt^{\bullet})_2]$, and $[Mo^{III}(abt^{\bullet})_3]$.

While we cannot discern unambiguously between these three possibilities crystallographically, it is clear at this point that a description as $[Mo^{VI}(L_{N,S})_3]$ or $[Mo^{VI}(abt)_3]$[14] each containing three amido-phenolate ligands, $(L_{N,S})^{2-}$ or $(abt)^{2-}$, and a molybdenum(VI) ion is inappropriate.

From the reaction of 3 equiv of the ligand 3,5-di-*tert*-butyl-1,2-benzenedithiol and 1 equiv of $[MoO_2(acac)_2]$ in methanol

(14) Yamaouchi, K.; Enemark, J. H. *Inorg. Chem.* **1978**, *17*, 2911.
(15) Ghosh, P.; Bill, E.; Weyhermüller, T.; Wieghardt, K. *J. Am. Chem. Soc.* **2003**, *125*, 3967.

Table 4. Bond Distances (Å) and Angles (deg) in **2** and **3**[a]

		2			
Mo(1)−S(1)	2.3600(5)	Mo(1)−S(21)	2.3709(5)	Mo(1)−S(41)	2.3645(6)
Mo(1)−S(2)	2.3677(5)	Mo(1)−S(22)	2.3602(5)	Mo(1)−S(42)	2.3582(6)
S(1)−C(1)	1.745(2)	S(21)−C(21)	1.748(2)	S(41)−C(41)	1.743(2)
S(2)−C(2)	1.738(2)	S(22)−C(22)	1.715(2)	S(42)−C(42)	1.733(2)
C(1)−C(2)	1.410(3)	C(21)−C(22)	1.414(3)	C(41)−C(42)	1.413(3)
C(1)−C(6)	1.433(2)	C(21)−C(26)	1.431(3)	C(41)−C(46)	1.436(3)
C(2)−C(3)	1.414(2)	C(22)−C(23)	1.404(3)	C(42)−C(43)	1.410(3)
C(3)−C(4)	1.376(2)	C(23)−C(24)	1.369(3)	C(43)−C(44)	1.371(3)
C(4)−C(5)	1.415(4)	C(24)−C(25)	1.413(3)	C(44)−C(45)	1.417(3)
C(5)−C(6)	1.381(2)	C(25)−C(26)	1.373(3)	C(45)−C(46)	1.384(3)
S(1)−Mo(1)−S(2)	81.42(2)				
S(21)−Mo(1)−S(22)	81.33(2)				
S(41)−Mo(1)−S(42)	81.65(2)				
S(1)−Mo(1)−S(41)	136.27(2)				
S(22)−Mo(1)−S(41)	132.92(2)				
S(42)−Mo(1)−S(21)	135.63(2)				
		3			
W(1)−S(1)	2.361(1)	W(1)−S(21)	2.360(1)	W(1)−S(41)	2.363(1)
W(1)−S(2)	2.374(1)	W(1)−S(22)	2.352(1)	W(1)−S(42)	2.357(1)
S(1)−C(1)	1.748(4)	S(21)−C(21)	1.773(4)	S(41)−C(41)	1.763(4)
S(2)−C(2)	1.738(4)	S(22)−C(22)	1.723(4)	S(42)−C(42)	1.739(4)
C(1)−C(2)	1.411(5)	C(21)−C(22)	1.391(6)	C(41)−C(42)	1.412(5)
C(1)−C(6)	1.428(5)	C(21)−C(26)	1.437(5)	C(41)−C(46)	1.429(45)
C(2)−C(3)	1.411(5)	C(22)−C(23)	1.413(6)	C(42)−C(43)	1.402(5)
C(3)−C(4)	1.375(5)	C(23)−C(24)	1.380(6)	C(43)−C(44)	1.371(5)
C(4)−C(5)	1.410(5)	C(24)−C(25)	1.408(6)	C(44)−C(45)	1.411(5)
C(5)−C(6)	1.377(5)	C(25)−C(26)	1.378(6)	C(45)−C(46)	1.380(5)
S(1)−W(1)−S(2)	81.11(3)				
S(21)−W(1)−S(22)	81.18(4)				
S(41)−W(1)−S(42)	81.39(3)				
S(1)−W(1)−S(21)	134.22(4)				
S(22)−W(1)−S(41)	133.86(4)				
S(1)−W(1)−S(41)	135.25(4)				

[a] Atom labels for **3** are the same as for $[Mo(L_{S,S})_3]$ shown in Figure 1.

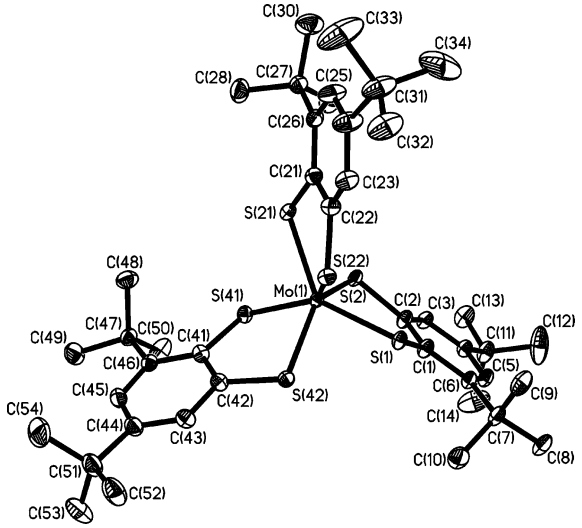

Figure 2. Structure of the neutral molecule $[Mo(L_{S,S})_3]^0$ in crystals of **2**. Thermal ellipsoids are drawn at the 50% level. The structure of $[W(L_{S,S})_3]$ in crystals of **3** is very similar and is not shown.

Table 5. Dihedral Bending Angles (deg) between Planes MS_2 and S_2 Phenyl

	α	α′	α″	α_{av}	ref
$[Mo(bdt)_3]^0$	13.1	21.1	30.0	21.4	2a
$[W(bdt)_3]^0$	13.5	22.6	32.1	22.7	2b
$[Mo(L_{S,S})_3]^0$	17.1	17.9	21.0	18.6	this work
$[W(L_{S,S})_3]^0$	18.3	19.0	23.9	20.4	this work
$[Mo(L_{S,S})_3]^-$	13.6	23.9	3.3	13.6	this work
$[W(L_{S,S})_3]^-$	11.9	21.2	4.4	12.5	this work
$[Mo(bdt)_3]^{2-}$	1.8	1.8	3.3	2.3	3b

(or WCl_6 in CCl_4), dark-bluish-green crystals of diamagnetic $[Mo(L_{S,S})_3]$ (**2**) (or $[W(L_{S,S})_3]$ (**3**), $S = 0$) were obtained in good yields.

Figure 2 displays the structure of the neutral molecule in crystals of **2**; that of $[W(L_{S,S})_3]$ in crystals of **3**·0.5CH_3CN is similar and not shown. Bond lengths and angles are given in Table 4. Complexes **2** and **3** are isostructural and isomorphous. Both complexes exhibit nearly ideal trigonal-prismatic geometry of their respective MS_6 polyhedra (Table 3). They resemble closely the geometries in neutral $[M(bdt)_3]$ (M = Mo, W)[2a,b], which indicates the absence of special packing forces in the solid state for the stabilization of the trigonal-prismatic geometry.

In Table 5, the dihedral bending angles α, α′, and α″ between the MS_2 plane and the S_2-phenyl ring plane of the $M(S_2C_6H_4)$ five-membered chelates are summarized. An irregular but strong bending is observed for the neutral $[M(bdt)_3]^0$ complexes (M = Mo, W). In **2** and **3**, the respective three angles of α, α′, and α″ are more regular

(16) Kirk, M. L.; McNaughton, R. L.; Helton, M. E. In *Progress in Inorganic Chemistry*; Stiefel, E. I., Ed.; John Wiley & Sons: Hoboken, NJ, 2004; Vol. 52, p 111
(17) Ray, K.; Weyhermüller, T.; Goossens, A.; Crajé, M. W.; Wieghardt, K. *Inorg. Chem.* **2003**, *42*, 4082.
(18) Petrenko, T.; Ray, K.; Wieghardt, K. E.; Neese, F. *J. Am. Chem. Soc.* **2006**, *128*, 4422.
(19) Fuggle, J. C. *Phys. Scr.* **1987**, *T17*, 64.
(20) (a) George, S. J.; Lowery, M. D.; Solomon, E. I.; Cramer, S. P. *J. Am. Chem. Soc.* **1993**, *115*, 2968. (b) Cramer, S. P.; deGroot, F. M. F.; Ma, Y.; Chen, C. T.; Sette, F.; Kipke, C. A.; Eichhorn, D. M.; Chan, M. K.; Armstrong, W. H. *J. Am. Chem. Soc.* **1991**, *113*, 7937. (c) Wasinger, E. C.; deGroot, F. M. F.; Hedman, B.; Hodgson, K. O.; Solomon, E. I. *J. Am. Chem. Soc.* **2003**, *125*, 12894.
(21) Ray, K.; DeBeer George, S.; Solomon, E. I.; Wieghardt, K.; Neese, F. *Chem.—Eur. J.* **2007**, *13*, 2783.
(22) (a) Szilagyi, R. K.; Lim, B. S.; Glaser, T.; Holm, R. H.; Hedman, B.; Hodgson, K. O.; Solomon, E. I. *J. Am. Chem. Soc.* **2003**, *125*, 9158. (b) Sarangi, R.; DeBeer George, S.; Rudd, D. J.; Szilagyi, R. K.; Ribas, X.; Rovira, C.; Almeida, M.; Hodgson, K. O.; Hedman, B.; Solomon, E. I. *J. Am. Chem. Soc.* **2007**, *129*, 2316.
(23) Cervilla, A.; Pérez-Pla, F.; Llois, E.; Piles, M. *Inorg. Chem.* **2005**, *44*, 4106.
(24) Cervilla, A.; Pérez-Pla, F.; Llopis, E.; Piles, M. *Inorg. Chem.* **2006**, *45*, 7357.

Table 6. Selected Bond Distances (Å) and Angles (deg) in the Monoanions of **4** and **5**

		4			
Mo(1)−S(1)	2.3733(7)	Mo(1)−S(21)	2.3824(7)	Mo(1)−S(41)	2.3733(7)
Mo(1)−S(2)	2.3818(8)	Mo(1)−S(22)	2.3911(7)	Mo(1)−S(42)	2.3560(7)
S(1)−C(1)	1.765(3)	S(21)−C(21)	1.759(3)	S(41)−C(41)	1.759(3)
S(2)−C(2)	1.751(3)	S(22)−C(22)	1.764(3)	S(42)−C(42)	1.744(3)
C(1)−C(2)	1.404(4)	C(21)−C(22)	1.407(4)	C(41)−C(42)	1.411(4)
C(1)−C(6)	1.417(4)	C(21)−C(26)	1.416(4)	C(41)−C(46)	1.430(4)
C(2)−C(3)	1.388(4)	C(22)−C(23)	1.401(4)	C(42)−C(43)	1.400(4)
C(3)−C(4)	1.387(4)	C(23)−C(24)	1.386(4)	C(43)−C(44)	1.373(4)
C(4)−C(5)	1.404(4)	C(24)−C(25)	1.404(4)	C(44)−C(45)	1.412(4)
C(5)−C(6)	1.396(4)	C(25)−C(26)	1.399(4)	C(45)−C(46)	1.392(4)
S(1)−Mo(1)−S(2)	81.21(2)				
S(21)−Mo(1)−S(22)	81.11(2)				
S(41)−Mo(1)−S(42)	81.69(3)				
S(1)−Mo(1)−S(21)	158.08(3)				
S(2)−Mo(1)−S(41)	159.37(3)				
S(42)−Mo(1)−S(22)	152.21(3)				
		5			
W(1)−S(1)	2.373(2)	W(1)−S(21)	2.380(2)	W(1)−S(1)	2.373(2)
W(1)−S(2)	2.376(2)	W(1)−S(22)	2.373(2)	W(1)−S(2)	2.376(2)
S(1)−C(1)	1.763(7)	S(21)−C(21)	1.763(7)	S(41)−C(41)	1.769(8)
S(2)−C(2)	1.743(8)	S(22)−C(22)	1.775(8)	S(42)−C(42)	1.754(8)
C(1)−C(2)	1.39(1)	C(21)−C(22)	1.40(1)	C(41)−C(42)	1.37(1)
C(1)−C(6)	1.41(1)	C(21)−C(26)	1.41(1)	C(41)−C(46)	1.43(1)
C(2)−C(3)	1.41(1)	C(22)−C(23)	1.41(1)	C(42)−C(43)	1.41(1)
C(3)−C(4)	1.38(1)	C(23)−C(24)	1.40(1)	C(43)−C(44)	1.35(1)
C(4)−C(5)	1.40(1)	C(24)−C(25)	1.38(1)	C(44)−C(45)	1.42(1)
C(5)−C(6)	1.39(1)	C(25)−C(26)	1.39(1)	C(45)−C(46)	1.36(1)
S(1)−W(1)−S(2)	81.59(7)				
S(21)−W(1)−S(22)	81.36(7)				
S(41)−W(1)−S(42)	81.61(8)				
S(1)−W(1)−S(21)	158.27(7)				
S(2)−W(1)−S(41)	159.62(7)				
N(42)−W(1)−S(22)	153.91(7)				

and support the notion that in the former solid-state packing forces are more important than in the bulky latter complexes.[16]

One-electron reduction of the neutral complexes in **2** and **3** with $[N(n\text{-}Bu)_4](SH)$ in CH_2Cl_2 solution under anaerobic conditions yields the paramagnetic ($S = {}^1/_2$) salts $[N(n\text{-}Bu)_4][Mo^V(L_{S,S})_3]$ (**4**) and $[N(n\text{-}Bu)_4][W^V(L_{S,S})_3]$ (**5**), respectively. Recrystallization from CH_3CN and CH_2Cl_2 solutions yielded suitable crystals of **4**·CH_3CN and **5**·$0.2CH_2Cl_2$ for X-ray crystallography, respectively.

Figure 3 shows the structure of the monoanion $[Mo^V(L_{S,S})_3]^-$ in crystals of **4**·CH_3CN; that of $[W^V(L_{S,S})_3]^-$ in crystals of **5**·$0.2CH_2Cl_2$ is very similar and not shown. The geometry of the MS_6 polyhedra in both monoanions is intermediate between trigonal-prismatic and octahedral ($\Theta_{av} = 31.7°$ and 31.5°, respectively; Table 3). The structure is very similar to those of $[M(bdt)_3]^-$ (M = Mo, W).[3,4] This is again taken as evidence that packing forces in the solid state are not important. We note that the structure of $[Mo^V(3,6\text{-dichloro-}1,2\text{-benzenedithiolato})_3]^-$ with $\Theta_{av} \sim 30°$ is also very similar.[6] The authors of ref 6 have noted that the geometry of the monoanions in the solid state is independent of the nature of the countercation.

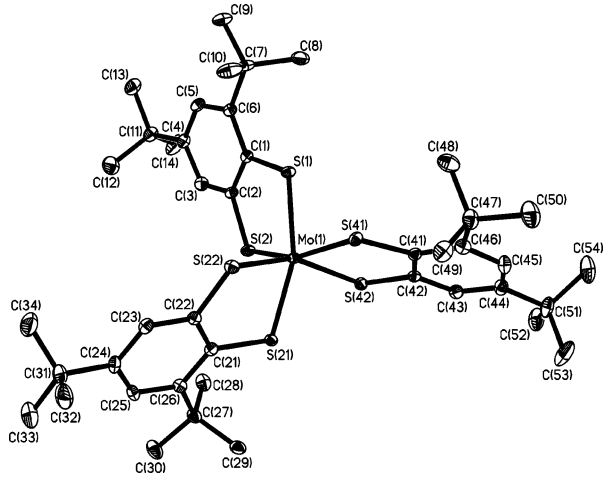

Figure 3. Structure of the monoanion $[Mo^V(L_{S,S})_3]^-$ in crystals of **4**·CH_3CN. Thermal ellipsoids are drawn at the 50% level. The structure of $[W^V(L_{S,S})_3]^-$ in crystals of **5**·$0.2CH_2Cl_2$ is very similar and is not shown.

Table 5 gives the bending angles of α, α′, α″ for the monoanions in **4** and **5**. They are irregular ranging from ∼3° to 24° in **4** and ∼4° to 21° in **5**.

Table 4 summarizes bond distances and angles of the neutral complexes in **2** and **3**; those for the monoanions in **4** and **5** are given in Table 6. It is interesting to compare the average Mo−S and C−S distances in **2** and **4**. The average Mo−S bond length in neutral **2** is 2.364 ± 0.002 Å; it is 2.376 ± 0.002 Å in the monoanion in **4**. Interestingly, the average C−S bond length is 1.737 ± 0.01 Å in **2** but longer at 1.757 ± 0.01 Å in **4**. This may indicate some ligand oxidation on going from **4** to **2** (or from **5** to **3**). It is not possible to use the above structural parameters for the unequivocal assignment of ligand vs metal-centered oxidations.

2. Spectro- and Electrochemistry. Cyclic voltammograms (CVs) of **1**, **2**, and **3** have been recorded in CH_2Cl_2 solutions containing 0.10 M $[N(n\text{-}Bu)_4]PF_6$ as supporting electrolyte at a glassy-carbon working electrode at 22 °C. The CVs are shown in Figure 4, and the potentials referenced vs the ferrocenium/ferrocene couple (Fc^+/Fc) are summarized in Table 7.

The CV of neutral **1** displays three reversible one-electron-transfer waves of which the first corresponds to an one-electron oxidation yielding the monocation $[\mathbf{1}]^+$ whereas the other two processes correspond to two successive one-electron reductions yielding the monoanion $[\mathbf{1}]^-$ and the dianion$[\mathbf{1}]^{2-}$, respectively.

Similarly, the CVs of **2** and **3** display two successive, reversible one-electron reductions yielding the monoanions $[\mathbf{2}]^-$ and $[\mathbf{3}]^-$ and the dianions$[\mathbf{2}]^{2-}$ and $[\mathbf{3}]^{2-}$, respectively.

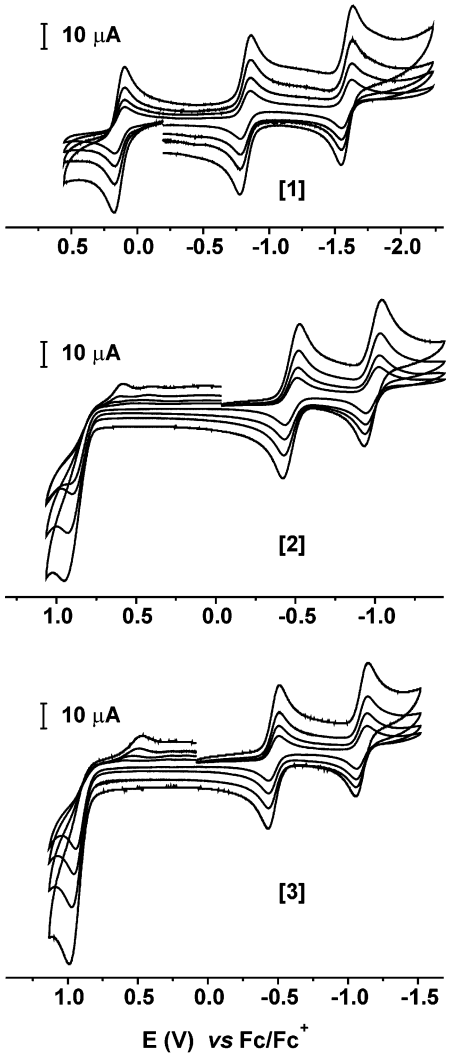

Figure 4. Cyclic voltammograms of **1** (top), **2** (middle), and **3** (bottom) in CH_2Cl_2 solution (0.10 M $[N(n\text{-}Bu)_4]PF_6$ at 22 °C). Conditions: 25, 50, 100, and 200 mV s^{-1} scan rates; glassy-carbon working electrode; redox potentials are referenced vs the Fc^+/Fc couple (ferrocene internal standard).

Table 7. Redox Potentials (V) of Complexes at 22 °C vs Fc^+/Fc

complex	$E^1_{1/2}$[a]	$E^2_{1/2}$[b]	$E^3_{1/2}$[c]
1	+0.13 r	−0.82 r	−1.50 r
2	+0.91 irr	−0.48 r	−0.99 r
3	+0.95 irr	−0.47 r	−1.11 r

[a] 1+/0 couple. [b] 0/1− couple. [c] 1−/2− couple (r = reversible; irr = irreversible).

The one-electron oxidations of **2** and **3** yielding the respective monocations $[\mathbf{2}]^+$and $[\mathbf{3}]^+$ are quasi- or irreversible and have not been studied in further detail.

Since the redox potentials are well separated from each other, we performed controlled potential electrolysis experiments to generate the oxidized monocation $[\mathbf{1}^+]$ and the mono- and dianionic reduced forms $[\mathbf{1}]^-$, $[\mathbf{2}]^-$, and $[\mathbf{3}]^-$ as well as $[\mathbf{1}]^{2-}$, $[\mathbf{2}]^{2-}$, and $[\mathbf{3}]^{2-}$ in solution and recorded their electronic spectra, which are shown in Figure 5 (top) for **1** with its oxidized and reduced forms, in Figure 5 (middle) for **2**, and in Figure 5 (bottom) for **3**. Their absorption maxima and extinction coefficients are summarized in Table 8.

Interestingly, the spectra of complexes$[\mathbf{1}]^+$ and **1** as well as those of **2** and **3** each display a very intense absorption maximum ($\epsilon > 1.5 \times 10^4$ M^{-1} cm^{-1}) in the near-infrared

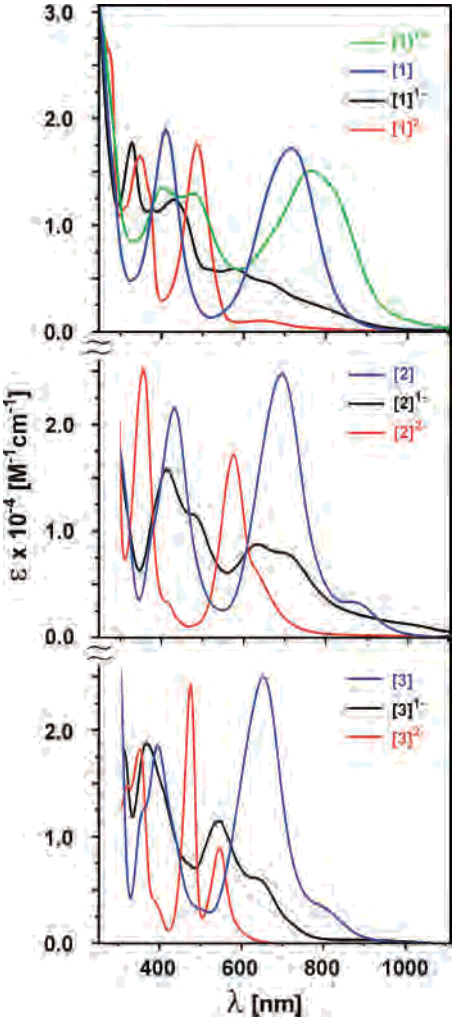

Figure 5. Electronic spectra of (a) **1** (blue), $[\mathbf{1}]^+$ (green), $[\mathbf{1}]^-$ (black), and $[\mathbf{1}]^{2-}$ (red) at the top; (b) **2** (blue), $[\mathbf{2}]^-$ (black), and $[\mathbf{2}]^{2-}$ (red) in the middle; and (c) **3** (blue), $[\mathbf{3}]^-$ (black), and $[\mathbf{3}]^{2-}$ (red) at the bottom. The monocation and the mono- and dianions were generated electrochemically at −5 °C.

Table 8. Electronic Spectra of Complexes in CH_2Cl_2 Solution (0.10 M $[N(n\text{-}Bu)_4]PF_6$) at −5 °C[a]

complex	λ_1 (ϵ_1)	λ_2 (ϵ_2)	λ_3 (ϵ_3)	λ_4 (ϵ)
1		408(2.04)	719(1.83)	
$[\mathbf{1}]^+$	402(1.42)	477(1.38)	767(1.60)	
$[\mathbf{1}]^-$	329(1.87)	438(1.31)	581(0.64)	663(0.51)
$[\mathbf{1}]^{2-}$	347(1.75)		486(1.88)	649(0.13)
2		430(2.14)	693(2.48)	881(0.32)
$[\mathbf{2}]^-$	413(1.57)	479(1.16)	638(0.88)	701(0.80)
$[\mathbf{2}]^{2-}$	353(2.5)	413(0.33)	575(1.71)	628(0.64)
3	353(1.25)	390(1.90)	649(2.53)	790(0.35)
$[\mathbf{3}]^-$	360(1.91)		537(1.17)	632(0.61)
$[\mathbf{3}]^{2-}$	344(1.84)	384(0.40)	468(2.45)	539(0.90)

[a] Wavelengths, λ, in nm, and extinction coefficients, ϵ, (10^{-4} M^{-1} cm^{-1}) in parentheses.

region (>600 nm), which we tentatively assign to an intervalence charge-transfer band (IVCT) between a $(L_{N,S})^{2-}$ or $(L_{S,S})^{2-}$ ligand and its one-electron oxidized π-radical $(L^{\bullet}_{N,S})^-$ or $(L^{\bullet}_{S,S})^-$. Such a maximum is a marker for the presence of ligand mixed valency.[17] These bands are absent in the mono- and dianions of **1**, **2**, and **3**.

We have also recorded the infrared spectra of **2** and **3** and of their monoanions $[\mathbf{2}]^-$ and $[\mathbf{3}]^-$ in a CH_2Cl_2 solution (0.10 M $[N(n\text{-}Bu)_4]PF_6$) in the range of 1200−1000 cm^{-1}. They are shown in Figure 6.

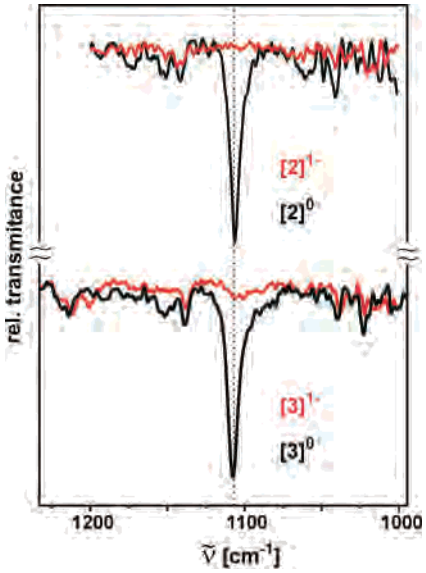

Figure 6. CH_2Cl_2 solution infrared spectra in the range 1200−1000 cm^{-1} of **2** (black) and its electrochemically generated monoanion $[\mathbf{2}]^-$ (red) at the top and **3** (black) and $[\mathbf{3}]^-$ (red) at the bottom.

Interestingly, both neutral complexes **2** and **3** display a strong $\nu(C{=}S^{\bullet})$ stretching frequency of an S,S-coordinated $(L^{\bullet}_{S,S})^-$ radical at 1106 cm^{-1}, whereas in the spectra of the reduced forms $[\mathbf{2}]^-$ and $[\mathbf{3}]^-$ this band is absent. They are also absent in the spectra of the dianions $[\mathbf{2}]^{2-}$ and $[\mathbf{3}]^{2-}$ (this is not shown).

The mode at ~1100 cm^{-1} has previously been identified as a marker for the presence of $(L^{\bullet}_{S,S})^-$ π radicals.[17,18] We note that in the IR spectra (KBr disks) of solid **2** and **4** only the former displays an intense $\nu(C{=}S^{\bullet})$ stretching frequency at 1117 cm^{-1} and, similarly, of **3** and **5** only the neutral complex **3** exhibits this stretching mode at 1117 cm^{-1}. This implies that the monoanions $[\mathbf{2}]^-$ and $[\mathbf{3}]^-$ contain three S,S-coordinated *o*-benzenedithiolato(2-) ligands, which renders the oxidation state of the central Mo or W ion +V, as has been suggested previously for the complexes $[M^{V}(bdt)_3]^-$ (M = Mo, W). In contrast, the neutral species **2** and **3** cannot be described as Mo^{VI} and W^{VI} species, respectively, containing three benzene-1,2-dithiolato(2-) ligands. Instead, a π-radical monoanion must be present, which enforces a +V oxidation state of the metal ions in **2** and **3**: $[Mo^{V}(L_{S,S})_2(L^{\bullet}_{S,S})]$ and $[W^{V}(L_{S,S})_2(L^{\bullet}_{S,S})]$. Both infrared and electronic absorption spectroscopy are in accord with only the latter proposal.

Thus, the electron-transfer series for **1** and **2** and for **3** involve the following species in eqs 2 and 3, respectively.

$$[Mo^{V}(L_{N,S})(L^{\bullet}_{N,S})_2]^+ \underset{-e}{\overset{+e}{\rightleftarrows}} [Mo^{V}(L_{N,S})_2(L^{\bullet}_{N,S})_2]^0 \underset{-e}{\overset{+e}{\rightleftarrows}} [Mo^{V}(L_{N,S})_3]^- \underset{-e}{\overset{+e}{\rightleftarrows}} [Mo^{IV}(L_{N,S})_3]^{2-} \quad (2)$$

$$[M^{V}(L_{S,S})_2(L^{\bullet}_{S,S})]^0 \underset{-e}{\overset{+e}{\rightleftarrows}} [M^{V}(L_{S,S})_3]^- \underset{-e}{\overset{+e}{\rightleftarrows}} [M^{IV}(L_{S,S})_3]^{2-} \quad (M = Mo, W) \quad (3)$$

3. X-ray Absorption Spectroscopy. Figure 7 displays the Mo L_2-edge X-ray absorption spectra (XAS) of solid samples

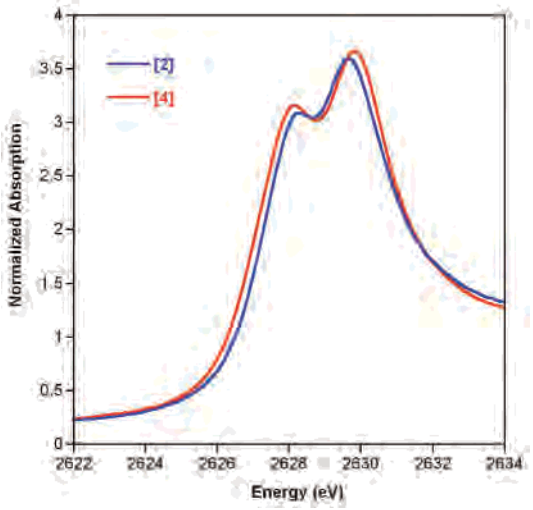

Figure 7. Comparison of the normalized Mo L_2-edge data for $[Mo^{V}(L^{\bullet}_{S,S})(L_{S,S})_2]$ (**2**) (blue) and $[Mo^{V}(L_{S,S})_3]^-$ (**4**) (red).

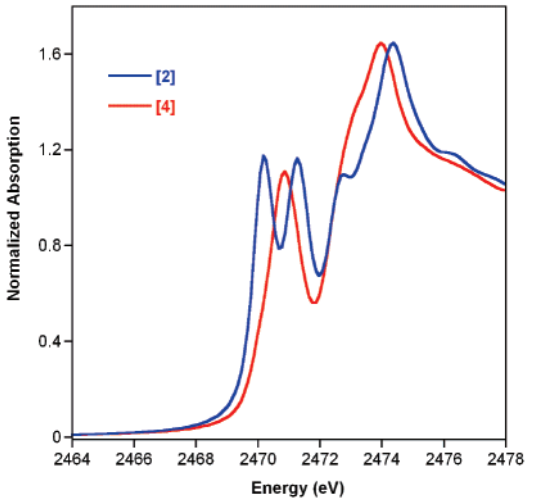

Figure 8. Comparison of the normalized S K-edge data for **2** (blue) and **4** (red).

of neutral, diamagnetic **2**, and paramagnetic **4**. The metal L edges result from the dipole-allowed 2p to 4d transition, which will split into L_3 and L_2 edges due to the spin−orbit coupling of the 2p hole.[19] The energies of these L_3 and L_2 transitions vary depending on the electronic structure of the site.[20] A change in the effective nuclear charge, Z_{eff}, due to a change in oxidation state (or in coordination number), will affect the energy of both the 2p and 4d orbitals.

Each spectrum in Figure 7 exhibits two peaks of very similar energies at 2628.2 and 2629.9 eV. This is a clear qualitative indication that the one-electron reduction of neutral $[Mo(L_{S,S})_3]^0$ (**2**) to the monoanion $[Mo(L_{S,S})_3]^-$ in **4** is not metal-centered. The oxidation states of the molybdenum ions in both **2** and **4** are identical, namely, +V.

In contrast, the S K-edge XAS data shown in Figure 8 for **2** and **4** and in Figure 9 for the tungsten analogue **3** (as compared with **2**) clearly show a remarkable difference between the respective neutral and its monoanionic counterpart.

The one-electron reduction of **2** yielding **4** and **3** affording **5** is a ligand-centered process involving the sulfur atoms.

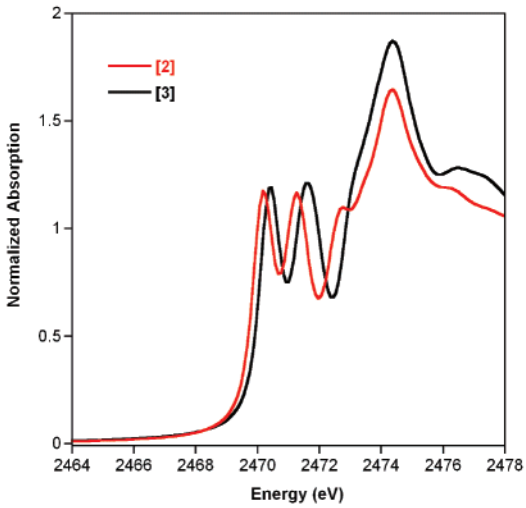

Figure 9. Comparison of the normalized S K-edge data for the neutral complexes **2** (red) and **3** (black).

The S K-edge spectrum of the monoanionic species in **4** displays an intense single pre-edge feature at ~2470.8 eV, which is typical for S,S′-coordinated, closed-shell benzene-1,2-dithiolates(2-).[21] On the other hand, the S K-edge spectra of the neutral species **2** and **3** both exhibit *two* pre-edge peaks, a lower-energy feature at ~2470.2 eV and a higher-energy feature, similar to the monoanionic species, at ~2471.3 eV. On the basis of the similarity of the Mo L_2-edge data for **2** and **4**, it is reasonable to assume that the higher-energy feature of the S K edges in neutral **2** corresponds to an S 1s transition to a primarily Mo 4d orbital. This transition is higher in energy in neutral **2** than in the monoanion in **4** because the increased effective nuclear charge on the sulfur moves the sulfur 1s orbital to a deeper binding energy and thus increases the overall transition energy. This is also reflected in the increase in the rising-edge energy. The lower pre-edge feature at 2470.2 eV is then assigned a S 1s to 3p transition reflecting ligand-radical character.[22]

Figure 9 shows a comparison of the S K-edge data for neutral **2** and **3**. The similarity of the two pre-edge peaks and the rising-edge structure of the two species indicates that both complexes have a similar electronic structure of the three dithiolate ligands involving at least one π-radical monoanion. Due to the extreme air-sensitivity of $[W(L_{S,S})_3]^-$ in **5**, it has not been possible to record reproducible X-ray absorption spectra at this point. However, the similarity of the infrared and electronic absorption spectra of **4** and **5** (and **2** and **3**) suggests that the tungsten complexes and the corresponding molybdenum species have the same electronic structures.

Conclusions

The most salient feature of this study is the discovery that the neutral tris(benzene-1,2-dithiolato)metal complexes of molybdenum and tungsten possess an electronic structure that is best described as $[M^V(L_{S,S})_2(L^{\bullet}_{S,S})]^0$ (M^V = Mo, W) containing a central Mo^V or W^V (d^1) ion, two diamagnetic, closed-shell dithiolato dianions, and a paramagnetic π-radical monoanion $(L^{\bullet}_{S,S})^-$ ($S_{rad} = {}^1/_2$). The spin of the π-radical anion is strongly antiferromagnetically coupled to the central metal ion yielding the observed diamagnetic ground state of **2** and **3**.

In contrast, the one-electron reduced monoanions in **4** and **5** contain a paramagnetic Mo^V or W^V ion and three closed-shell ligand dianions $(L_{S,S})^{2-}$.

Spectroscopic markers for the presence of the π radical in **2** and **3** are as follows: (1) The S K-edge spectra display a characteristic energy transition at ~2470.2 eV, which is absent in **4** and **5**. (2) In the infrared spectra of **2** and **3**, an intense $\nu(C{=}S^{\bullet})$ stretching frequency is observed at 1117 cm^{-1}, which again is absent in the spectra of **4** and **5**. (3) The electronic spectra of **2** and **3** display an intense IVCT band in the near-infrared region at 881 nm ($\epsilon = 0.32 \times 10^4$ M^{-1} cm^{-1}) and 790 nm ($\epsilon = 0.35 \times 10^4$ M^{-1} cm^{-1}), respectively. This IVCT band is absent in **4** and **5**.

The above results call for a reinterpretation of some recently reported chemistry of $[Mo(bdt)_3]$ and $[W(bdt)_3]$[23,24] of which the most interesting aspect is the claim that these neutral complexes oxidize water or phosphines (eqs 4 and 5).

$$2[Mo^{VI}(S_2C_6H_4)_3] + H_2O \rightarrow 2[Mo^{V}(S_2C_6H_4)_3]^- + 2H^+ + {}^1/_2O_2 \quad (4)$$

$$2[Mo^{VI}(S_2C_6H_4)_3] + H_2O + PPh_3 \rightarrow 2[Mo^{V}(S_2C_6H_4)_3]^- + 2H^+ + OPPh_3 \quad (5)$$

The proposed mechanisms invoke a seven-coordinate intermediate $[(OH)Mo^{VI}(S_2C_6H_4)_3]^-$, which according to our results is unlikely to exist.

Acknowledgment. We are grateful to the Fonds der Chemischen Industrie for financial support of this work. R.K. thanks the Max-Planck Society for a stipend. SSRL operations are funded by the Department of Energy, Office of Basic Energy Sciences. The Structural Molecular Biology program is supported by the National Institutes of Health, National Center for Research Resources, Biomedical Technology Program, and by the Department of Energy, Office of Biological and Environmental Research.

Supporting Information Available: X-ray crystallographic files in CIF format for **1**−**5**. This material is available free of charge via the Internet at http://pubs.acs.org.

IC700600R